doi: 10.5028/jatm.2010.02038810

Rogério Pirk*
Institute of Aeronautics and Space
São José dos Campos – Brazil
rogeriorp@iae.cta.br

Carlos d'Andrade Souto
Institute of Aeronautics and Space
São José dos Campos – Brazil
carloscdas@iae.cta.br

Dimas Donizeti da Silveira
Institute of Aeronautics and Space
São José dos Campos – Brazil
dimasdds@iae.cta.br

Cândido Magno de Souza
Institute of Aeronautics and Space
São José dos Campos – Brazil
candidocms@iae.cta.br

Luiz Carlos Sandoval Góes
Technological Institute of Aeronautics
São José dos Campos – Brazil
goes@ita.br

*author for correspondence

Liquid rocket combustion chamber acoustic characterization

Abstract**:** *Over the last 40 years, many solid and liquid rocket motors have experienced combustion instabilities. Among other causes, there is the interaction of acoustic modes with the combustion and/or fluid dynamic processes inside the combustion chamber. Studies have been showing that, even if less than 1% of the available energy is diverted to an acoustic mode, combustion instability can be generated. On one hand, this instability can lead to ballistic pressure changes, couple with other propulsion systems such as guidance or thrust vector control, and in the worst case, cause motor structural failure. In this case, measures, applying acoustic techniques, must be taken to correct/minimize these influences on the combustion. The combustion chamber acoustic behavior in operating conditions can be estimated by considering its behavior in room conditions. In this way, acoustic tests can be easily performed, thus identifying the cavity modes. This paper describes the procedures to characterize the acoustic behavior in the inner cavity of four different configurations of a combustion chamber. Simple analytical models are used to calculate the acoustic resonance frequencies and these results are compared with acoustic natural frequencies measured at room conditions. Some comments about the measurement procedures are done, as well as the next steps for the continuity of this research. The analytical and experimental procedures results showed good agreement. However, limitations on high frequency band as well as in the identification of specific kinds of modes indicate that numerical methods able to model the real cavity geometry and an acoustic experimental modal analysis may be necessary for a more complete analysis. Future works shall also consider the presence of passive acoustic devices such as baffles and resonators capable of introducing damping and avoiding or limiting acoustic instabilities.*

Keywords: *Combustion chamber, Combustion instability, Acoustic resonance, Liquid rocket engine (LRE).*

INTRODUCTION

Combustion instabilities have been present in the development of liquid rocket engines (LRE) over the last decades. There are basically three types of combustion instabilities in LRE: low frequency, medium frequency and high frequency. Low frequency instabilities, also called chugging, are caused by pressure interactions between the propellant feed system and the combustion chamber. Medium frequency instabilities, also called buzzing, are due to coupling between the combustion process and the propellant feed system flow. The high frequency instabilities are the most potentially dangerous and not well-understood ones. It occurs due to coupling of the combustion process and the chamber acoustics (Sutton and Biblarz, 2001).

The presence of acoustic (high frequency) combustion instabilities shall be considered still in development phase, although only after real firing tests combustion instabilities can be clearly identified.

Combustion chambers environments present high levels of acoustic noise. Bunrley and Culick (1997) described that this can be verified when the power spectrum of the acoustic pressure levels, measured during burning tests of the chambers, is analyzed. When an oscillation is observed, i.e., combustion instability, sound pressure peaks with well-defined magnitudes summed to the background noise are present. These peaks are correlated with the resonance frequencies of the combustion chambers cavities, where the sound pressure on each position of the acoustic fluid space represent the environment oscillation, attributed to the acoustic modes of these cavities. Such a way occurs the coupling of the acoustic natural frequencies and the burning oscillations of the combustion chamber, which can cause instabilities and consequent unexpected behavior such as efficiency loss or even explosion of the engine.

A LRE combustion chamber has longitudinal, tangential and radial acoustic modes. Coupled modes combining

Received: 14/09/10
Accepted: 20/10/10

these types are also possible to occur. The tangential and radial modes are the most dangerous to high frequency instabilities (Yang, Wicker and Yoon, 1994). The three basic types of acoustic modes of a cylinder representing a LRE combustion chamber are shown in Fig. 1.

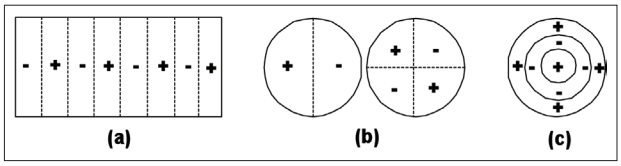

Figure 1: Longitudinal (a), tangential (b) and radial modes (c).

Some works showed that the acoustic behavior of a combustion chamber is weakly affected by the combustion process. Comparing to room pressure and temperature conditions, the chamber cavity mode shapes remain basically the same, but its eigenfrequencies are shifted, actually multiplied by a number defined by the ratio of sound speed velocity at real operation temperature and at room temperature (Laudien et al., 1994).

In the development of a liquid rocket engine of 75 KN thrust by the Institute of Aeronautics and Space (IAE), the acoustic behavior of the combustion chamber is being considered. An investigation of some different combustion chambers is proposed. These studies may be done in two steps, using theoretical calculation and experimental measurements. As such, theoretical and experimental natural frequencies of the acoustic cavity are obtained, and a comparison/validation of the mathematical model can be done.

First, considering the geometry of the combustion chamber and the physical parameters of air, natural frequencies of this cavity are calculated theoretically. The acoustic frequencies can also be obtained by using a test setup to measure the sound pressure levels of this acoustic domain.

A third possible method to obtain the acoustic behavior of combustion chambers is by modeling the cavity using numerical methods such as the Finite Element Method (FEM) or the Boundary Element Method (BEM). As such, by applying virtual prototypes' techniques, besides calculating the resonance, the associated acoustic mode shapes are obtained. With these three methods, theoretical *versus* experimental comparisons can be carried out for the validation of the existing models.

Since a combustion acoustic instability (and the acoustic mode to which it is related) is identified, some measures can be taken to avoid or minimize it. Some design parameters in the combustion chamber and injector play an important role in high frequency combustion instabilities. By changing these parameters, one can obtain a design less susceptible to this kind of instabilities (Huzel and Huang, 1992). Also, passive acoustic devices for the attenuation of acoustic noise, as Helmholtz resonators, liners, baffles and ¼ wave filters can be introduced in the combustion chamber (Santana Junior et al., 2009).

It is important to mention that, in the latter stages of this survey, numerical methods for modeling acoustics of chambers as well as insulation treatments for attenuating acoustic noises will be presented. Currently, only comparisons between theoretical *versus* experimental results, using simple mathematical models and measured frequency response functions, respectively, are carried out for different configurations of a combustion chamber.

OBJETIVE

The objective of this work was to present the adopted procedures for the dynamic characterization of different configurations of combustion chamber models for a liquid rocket engine capable of generating 75 kN thrust. The models were built on aluminum, in 1:1 scale. In order to assess the influence of the chamber geometry on the chamber acoustic behavior, the referred combustion chamber models were segmented. This segmentation allowed us analyzing the influence of the different lengths on the dynamic behavior of the acoustic environment. It is worth mentioning that the tests were performed under room environmental conditions, without simulating the pressure and temperature conditions during the combustion of a rocket engine.

Hereinafter, the measurement procedures to obtain the acoustic parameters of different configurations of the 75 kN combustion chamber, as well as the method applied for the calculation of the theoretical natural frequencies were presented. Measuring setup, collected data and the applied criteria for the choice of FRF were described, as well as the results obtained. Theoretical *versus* experimental comparisons, for the different configurations, are done and the reliability of the formulation applied to calculate the analytical resonances is verified.

PROCEDURES AND METHODOLOGIES

As it was mentioned before, the experimental determination of the acoustic characteristics of combustion chambers was performed in room conditions, i. e., without considering the burning conditions inside the combustion chamber cavity as mixing of gasses, temperature, pressure, mass density etc.

A mock up of the 75 kN LRE was built on aluminum, with the possibility of assembling different parts, thus creating many configurations of the referred engine. Figure 2 shows

the 75 kN LRE, which was segmented in order to assess the inner combustion chamber dynamic behavior considering different configurations, including the different sizes of the nozzle. In other words, such segmentation allows verifying the influence of the different geometries on the acoustic behavior of the chamber cavity, which is an important source of combustion instability. The measured acoustic parameters of each configuration may be compared with the respective parameters, calculated by a mathematical model.

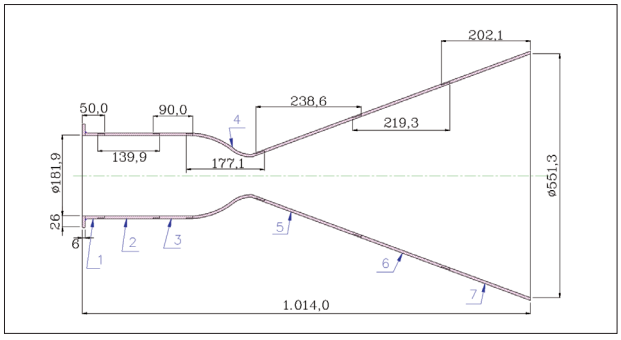

Figure 2: Dimensions of the segmented combustion chamber in millimeters.

Note in Fig. 2 that it is possible to built 16 configurations for the 75 kN LRE. Even though it is possible to assemble such different configurations, this paper describes the analysis performed only for the configurations B1, B2, C1 and D1. As such, the influences of the internal volume and length of the combustion chamber as well as the size of the nozzle are assessed.

Figure 3 presents all the possible configurations, with and without nozzle, including variations of the volume of the combustion chamber and the size of the nozzle.

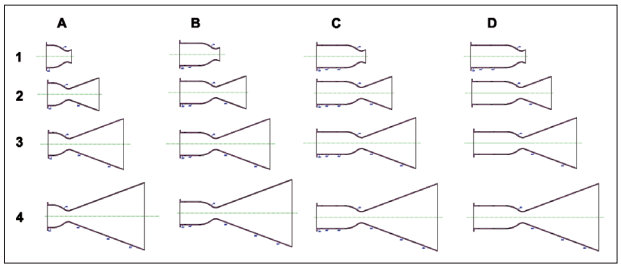

Figure 3: Different configurations of the 75 kN LRE.

Table 1 describes, for each configuration, the connected segments to build up the different geometries of the combustion chamber. The numbers presented on the referred table represent the segments denoted in Fig. 2.

THEORETICAL CALCULATIONS

Equation 1 describes the considered mathematical model for the acoustic natural frequencies calculation of the set of configurations. The inner acoustic environment is treated as an acoustically closed system, even though the nozzle is in contact with the external fluid or external acoustic environment. Such approximation has showed good theoretical *versus* experimental agreement (Laudien et al., 1994).

$$f_{lmn} = \frac{c}{2\pi}\sqrt{\frac{\lambda_{mn}^2}{R_c^2} + \frac{k^2\pi^2}{L_c^2}} \qquad (1)$$

where:

c: speed of sound;

λ: transversal eigenvalue, for m,n = 0,1,2... (Laudien et al., 1994);

k, m, n = 0,1,2... longitudinal, tangential and radial mode number directions;

R_c: combustion chamber radius;

L_c: effective acoustic length (distance between injectors faceplate and nozzle throat, less approximately one-half of the converging nozzle length).

Note that in Eq. 1 the modes and its associated natural frequencies are function of the chamber geometry and the three orthogonal directions k, m and n. Table 2 gives the calculated values, assuming the temperature of the air 20ºC, universal gas constant at pressure and volume constants ($\gamma = {}^{c_p}\!/_{c_v} = 1.4$), which yields speed of sound c = 343 m/s.

Table 1: Sequence of segments to be connected for each configuration

CFG*	Segments	CFG*	Segments	CFG*	Segments	CFG*	Segments
A1	1-4	B1	1-2-4	C1	1-2-3-4	D1	1-2-2-4
A2	1-4-5	B2	1-2-4-5	C2	1-2-3-4-5	D2	1-2-2-4-5
A3	1-4-5-6	B3	1-2-4-5-6	C3	1-2-3-4-5-6	D3	1-2-2-4-5-6
A4	1-4-5-6-7	B4	1-2-4-5-6-7	C4	1-2-3-4-5-6-7	D4	1-2-2-4-5-6-7

* Segments are shown in Figure 2.

Table 2: Calculated acoustic natural frequencies

Acoustic mode	Orthogonal directions			λ	Configurations			
	k	m	n	transversal	CFG B1	CFG B2	CFG C1	CFG D1
1st long	1	0	0	0	717.812	717.812	546.3603	471.3108
2nd long	2	0	0	0	1435.625	1435.625	1092.721	942.6216
3rd long	3	0	0	0	2153.437	2153.437	1639.081	1413.932
1st tang	0	1	0	1.8412	1105.493	1105.493	1105.493	1105.493
2nd tang	0	2	0	3.0542	1833.803	1833.803	1833.803	1833.803
1st radial	0	0	1	3.8317	2300.63	2300.63	2300.63	2300.63
2nd radial	0	0	2	7.0156	4212.307	4212.307	4212.307	4212.307
1st rad/1st tang	0	1	1	5.3314	3201.079	3201.079	3201.079	3201.079
1st rad/2nd tang	0	2	1	6.7061	4026.477	4026.477	4026.477	4026.477
2nd rad/1st tang	0	1	2	8.5363	5125.366	5125.366	5125.366	5125.366

EXPERIMENTAL MEASUREMENTS

For the experimental procedure, a noise source was positioned inside the combustion chamber close to the injectors face plate. A microphone was placed in many different positions into the combustion chamber cavity. The microphone measured the acoustic pressure response due to the noise in some points.

For each microphone position, Frequency Response Functions (FRF) measurements were taken, performing azimuthal swept at each 45º, positioning the microphone in the radial direction at distances 10 mm, 40 mm and 70 mm from the structure wall, and also performing an axial swept at each 50 mm. Figure 4 shows the position points to obtain the complete set of measurement data.

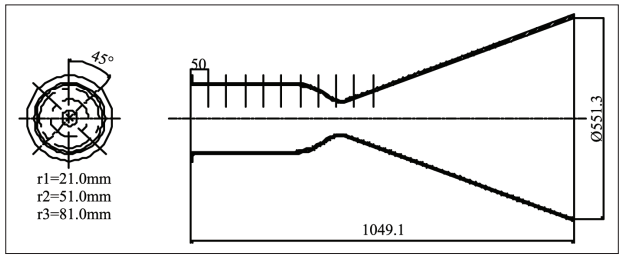

Figure 4: Microphones positioning.

Note that this measurement procedure generates a large amount of experimental data, since transversal data were measured at each 45º, positioned at 10 mm, 40 mm and 70 mm from the structure wall, taking as reference, the geometric center of the combustion chamber. Besides, axial measurements were performed at each 50 mm, up to 450 mm, depending on the chamber length.

After a first analysis, the results indicated that an optimized measuring procedure could be adopted, since the FRF presented similar behavior when they were acquired on the same plane, perpendicular to the direction of the wave propagation. For such optimization, one considered that the structural part of the combustion chamber is rigid and that the propagating acoustic waves in the inner acoustic environment of the combustion chamber assume a nearly acoustic plane wave or one-dimensional wave behavior. Such a way, the amount of measurements and data analysis for the next configurations can be decreased.

Acoustic plane waves are the simplest type of propagating waves through the fluid medium. The characteristic property of such waves is that parameters such as acoustic pressure, particle displacements etc., have the same amplitude on all points of any plane, perpendicular to the direction of propagation. As an example, the propagating waves in a confined fluid, through a rigid tube, generated by a vibrating piston, positioned at one of the edges of the tube. Any divergent type of wave, in a homogeneous medium, also assumes the characteristics of a plane wave, when it propagates at long distances from its source (Gerges, 1994). An important remark about the acoustic plane waves is that they have characteristics similar to those presented by the longitudinal waves propagating in a bar. Consequently, it is possible to deduce the wave equation through a fluid media, in which it is admitted being confined in a rigid tube, with constant transversal section (Burnley and Culick, 1997).

As such, the survey of the configurations B1, B2, C1 and D1 can define the optimization procedure for the next experiments, since some transversal measurement positions can be eliminated, assuming the plane wave behavior.

MEASUREMENT OF THE ACOUSTIC PARAMETERS

On these experimental assessments, the combustion chamber cavities were equipped with an external acoustic

source, installed at the injection faceplate of the engine, which injected an excitation noise inside the acoustic cavity. This noise was generated by a signal generator, which provided the white noise (0 to 20 kHz) to be injected by the noise source. However, due to practical manufacturing characteristics of the referred acoustic source, the spectral content of the injected noise inside the chamber cavity was from 400 Hz to 20 kHz.

The acquired FRF, describe the acoustic response of the fluid media (acoustic cavity) due to the external acoustic excitation. These FRF were captured by a ¼" capacitive pressure microphone, which was mounted on a thin rod, and with which it was possible to reach all the measurement positions, axial, azimuth and radial, in the chamber inner environment. This microphone was conditioned by power supply and preamplifier to measure the sound pressure level inside the combustion chamber, when it is subjected to an external acoustic excitation. The measured acoustic pressure levels were registered by using a digital analyzer, for posterior analysis. Figure 5 shows the measurement setup.

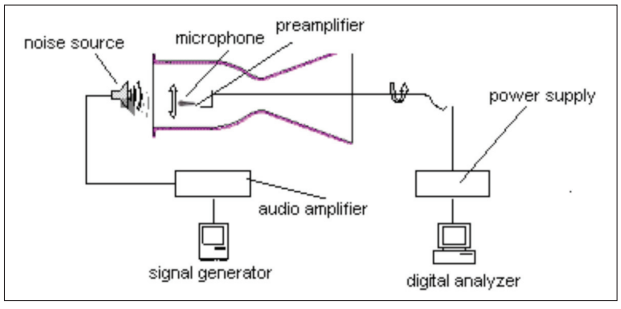

Figure 5: Measurement set up.

It is important to mention that this technique assumes linear behavior of the acoustic cavity. As such, the inherent dynamic characteristics of the combustion chamber are independent of the excitation type and its spectral components. Therefore, the dynamic behavior of an acoustic environment is the same for different excitations.

As described on Table 2, longitudinal, radial, axial, as well as coupled modes frequencies must be measured, to obtain a complete experimental data set, which contains all the acoustic FRF, to be compared with the referred theoretical frequencies. Then, it is important to measure the required acoustic traveling waves, by positioning the microphone in the correct direction, according to the transverse or axial measurement axe. As a pressure type microphone was used, it was important to place the sensor diaphragm perpendicularly to the direction of the propagating wave.

It is expected that the propagating waves inside the combustion chamber have a plane wave behavior, as described by Gerges (1994). This behavior can be verified when acoustic FRF in all points of a same plane, perpendicular to the direction of the wave propagation, may not present significant differences. As such, with the test results, this behavior could be verified and the experimental data points could be decreased, thus reducing the data to be analyzed.

RESULTS

Resonant frequencies of the combustion chamber were identified by analyzing the registered FRF (from 0 to 5,000 Hz), which were measured along the cavity of the chamber. Once identified, these frequencies were compared with the respective values, calculated theoretically (Table 2). As for each configuration, the theoretical frequencies were known, an experimental procedure of frequencies separation was performed by observing its value proximity (close to those calculated) and the higher amplitude (also considering the transversal/axial position of the microphone). Then, for each configuration, the acquired FRF were analyzed and the average of the frequencies and magnitudes was evaluated, by using the transversal and axial measurements, in order to obtain the set of resonant frequencies of the referred cavity. Such a way, with the theoretical *versus* experimental comparison, one can have an idea of the inherent acoustic mode shapes in the cavity, associated with the resonance frequencies.

Nevertheless, it is important to highlight that this frequency separation method can still be improved, once the simple theoretical *versus* experimental frequency comparison is not sufficiently accurate, considering that the mathematical model is a simple model of the acoustic cavity of the combustion chamber, with some approximations. As such, a manner of confirming the calculated mode shapes is performing acoustic modal analysis of the cavity to have all the acoustic modal parameters of the cavities. This technique will be applied in further studies. Figures 6, 7, 8 and 9 show the configurations during test for FRF measurements.

Figure 6: Configuration B1.

Figure 7: Configuration C1.

Figure 8: Configuration D1.

Figure 9: Configuration B2.

As the mathematical model assumes an acoustically closed environment, the influence of the nozzle was also verified. Tables 3, 4, 5 and 6 describe the identified experimental and calculated natural acoustic frequencies. These data are compared and an estimate of the error is described. The average magnitudes are also described.

The natural frequencies described on the referred tables were obtained by calculating averages of all measured values, as well as the identified resonances, visualized on FRF.

As mentioned before, the value proximity criterion is an inaccurate procedure. This can be confirmed, mainly in the higher frequency bands, where the FRF present large quantity of peaks (high modal density) and the frequency separation becomes a difficult task.

One still may consider that higher orders mathematical models are inaccurate, which present inherent acceptable errors, only for a few modes in the low frequency band. Observe the Tables 3, 4, 5 and 6 and verify that the error increases as a function of frequency. It is important to mention that the adopted measurement setup (number of points) for an acquisition up to 5,000 Hz introduces a bias error in the frequency domain of 6 Hz, approximately. This is another indication that a stochastic treatment is a method more appropriated to identify natural frequencies, since different measurement points and significant bias error may be considered.

DISCUSSION

Although the natural frequency determination procedure, using a simple mathematical model and considering the fluid room environmental conditions of temperature and pressure, gives a reasonable indication of its dynamic characteristics, it can still be improved to yield more accurate results. These first studies were useful, mainly for establishing an optimized measurement procedure, since the propagating plane wave behavior can be assumed for such experiment. As such, for other configurations, some transversal measurement points can be suppressed.

Note on Table 2 that the adopted mathematical model (Equation 1) calculated the same values of radial, tangential and coupled natural frequencies for all the configurations of the combustion chamber. This is due to the fact that these calculations take into account parameters as radial and transversal eigenvalues ($\lambda_{m,n}$) and radius of the combustion chamber (R_c), which have the same values for the referred configurations. Then, it means that there are no differences in the input data of the Equation 1. Therefore, the calculated axial or longitudinal natural frequencies for the configurations B1, C1 e D1 present different results, since these calculations are done by considering the mode number in the longitudinal direction (k), as well as the effective length of the chamber (L_c), which is function of the

Table 3: Experimental results and theoretical *versus* experimental comparison (B1)

Acoustic mode	Experimental natural frequency (Hz)	Theoretical natural frequency (Hz)	Error (%)	Mean value (dB)
1st longitudinal	719.0	717.812	0.1	110.0
2nd longitudinal	1272.3	1435.625	12.8	95.0
3rd longitudinal	2380.6	2153.437	9.5	105.0
1st tangential	1137.5	1105.493	2.8	86.0
2nd tangential	1793.2	1833.803	2.2	85.0
1st radial	2583.6	2300.63	11.0	107.0
2nd radial	4351.6	4212.307	3.2	90.0
1st radial/1st tangential	3237.2	3201.079	1.1	98.0
1st radial/2nd tangential	4456.7	4026.477	9.6	83.0
2nd radial/1st tangential	4744.3	5125.366	8.0	93.0

Table 4: Experimental results and theoretical *versus* experimental comparison (B2)

Acoustic mode	Experimental natural frequency (Hz)	Theoretical natural frequency (Hz)	Error (%)	Mean value (dB)
1st longitudinal	718.231	717.8123	0.01	106.40
2nd longitudinal	1311.623	1435.625	9.00	92.34
3rd longitudinal	2357.355	2153.437	8.60	105.68
1st tangential	1138.944	1105.493	2.90	88.30
2nd tangential	1875.003	1833.803	2.20	92.73
1st radial	2545.043	2300.63	9.60	101.59
2nd radial	4446.734	4212.307	5.30	98.50
1st radial/1st tangential	3267.713	3201.079	2.00	101.98
1st radial/2nd tangential	4333.683	4026.477	7.10	96.43
2nd radial/1st tangential	4515.181	5125.366	13.50	97.87

Table 5: Experimental results and theoretical *versus* experimental comparison (C1)

Acoustic mode	Experimental natural frequency (Hz)	Theoretical natural frequency (Hz)	Error (%)	Mean value (dB)
1st longitudinal	568.5	546.3603	3.9	110.8
2nd longitudinal	1039.3	1092.721	5.2	100.0
3rd longitudinal	1452.2	1639.081	12.8	90.0
1st tangential	1050.0	1105.493	5.3	100.9
2nd tangential	2253.8	1833.803	18.6	102.2
1st radial	2461.4	2300.63	6.5	100.7
2nd radial	4331.1	4212.307	2.7	95.6
1st radial/1st tangential	2964.6	3201.079	3.1	100.2
1st radial/2nd tangential	4086.3	4026.477	1.4	91.6
2nd radial/1st tangential	4715.2	5125.366	8.7	94.9

Table 6: Experimental results and theoretical *versus* experimental comparison (D1)

Acoustic mode	Experimental natural frequency (Hz)	Theoretical natural frequency (Hz)	Error (%)	Mean value (dB)
1st longitudinal	494.27	471.3108	4.6	107.64
2nd longitudinal	915.72	942.6216	2.9	102.35
3rd longitudinal	1265.07	1413.932	11.7	92.74
1st tangential	-----	1105.493	-----	-----
2nd tangential	2341.19	1833.803	21.7	103.54
1st radial	2426.16	2300.63	5.2	103.82
2nd radial	4409.29	4212.307	4.5	98.86
1st radial/1st tangential	3075.17	3201.079	4.1	99.96
1st radial/2nd tangential	4058.48	4026.477	0.7	95.78
2nd radial/1st tangential	4816.07	5125.366	6.4	96.97

studied geometries. It is important to consider that configurations B1 and B2 present the same natural frequencies, since the considered acoustic effective length is the same for both configurations. Note in Fig. 1 and Fig. 2 that these configurations are different only by the nozzle segmentation in B2, which may have investigated its influence on the dynamic behavior of the acoustic cavity.

Table 3, regarding B1, shows that the comparison of the natural frequencies does not present significant errors for the longitudinal modes. It can be noted that the approximation of the first longitudinal frequency, calculated by the theoretical model, presents good correlation with the measured value (0.1% error). The second and third longitudinal eigenvalues present 12.8 and 9.5%, respectively.

Figure 10 shows a FRF, measured in axial direction, with the microphone positioned at 100 mm. Observe the curve below and verify that the first frequency of 719 Hz and the third of 2,380 Hz, are easily identified, since they present magnitudes higher than 100 dB, while the second frequency of 1,272 Hz presents a 95 dB magnitude, approximately. Comparison of the tangential frequencies, despite the low acoustic pressure levels obtained on the calculations of the averaged magnitude (around 85 dB), also presented excellent agreement between the calculated values and those measured.

Concerning the two radial frequencies, the percent errors were 11 and 3%, respectively. These are significant errors, since the mathematical approximations usually present higher errors for the higher orders' modes, what is not the case. Still on Table 3, the coupled modes present errors of 1.1%, 9.6% and 8%, respectively.

On Table 4, corresponding to configuration B2, it is verified that the experimental values also present good correlation with the values obtained by mathematical approximation. The calculated error for the first longitudinal natural frequency is very small (<0.05%). The other longitudinal frequencies presented 9.0 and 8.6% error, respectively. Tangential comparisons also presented excellent correlation, with 2.9 and 2.2 %. It can also be seen that first, second and third coupled modes presented 2.0%, 7.1% and 13.5% errors, respectively. For the radial frequencies, the calculated differences were 9.6 and 5.3%. Figure 11 shows the measured FRF, with microphone positioned in transversal direction, at 10 mm from the structure wall, 0º azimuth and 100 mm distance from the sound source.

For the configuration C1, the comparisons are described on Table 5. Considering the longitudinal frequencies, it is verified that the results present a good correlation for the first and second resonances, since the calculated errors are 3.9 and 5.2%, respectively, with the measured magnitudes of 110 and 100 dB. The resonance of the inner environment due to the third longitudinal acoustic mode presented 12.8% error, with magnitude of 90 dB. Tangential frequencies also present an excellent agreement. Note the errors of 2.8 and 2.2%, respectively, for the two tangential natural frequencies of the configuration C1.

Concerning the radial resonances, the errors were 11%, at the frequency of 2,583 Hz (first radial mode) and 3%, for the frequency of 4,351 Hz (second radial mode). The coupled frequencies presented 10.4%, 9.6% and 8%, respectively.

Table 6 presents the comparisons concerning the configuration D1. Observe this table and note that, as

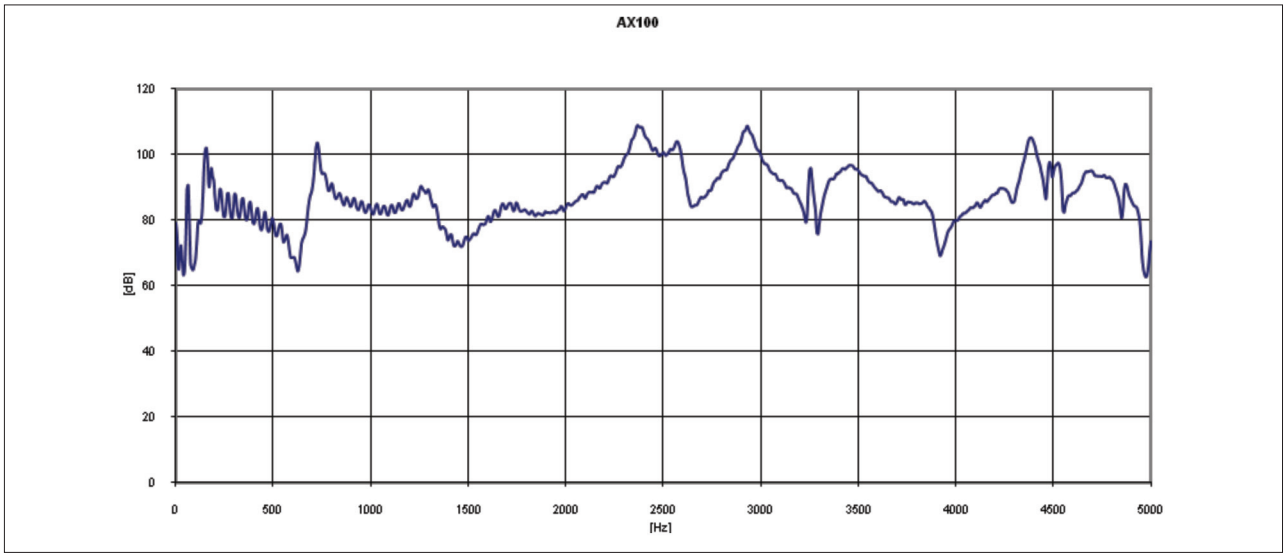

Figure 10: Axial measurement – Configuration CFGB1.

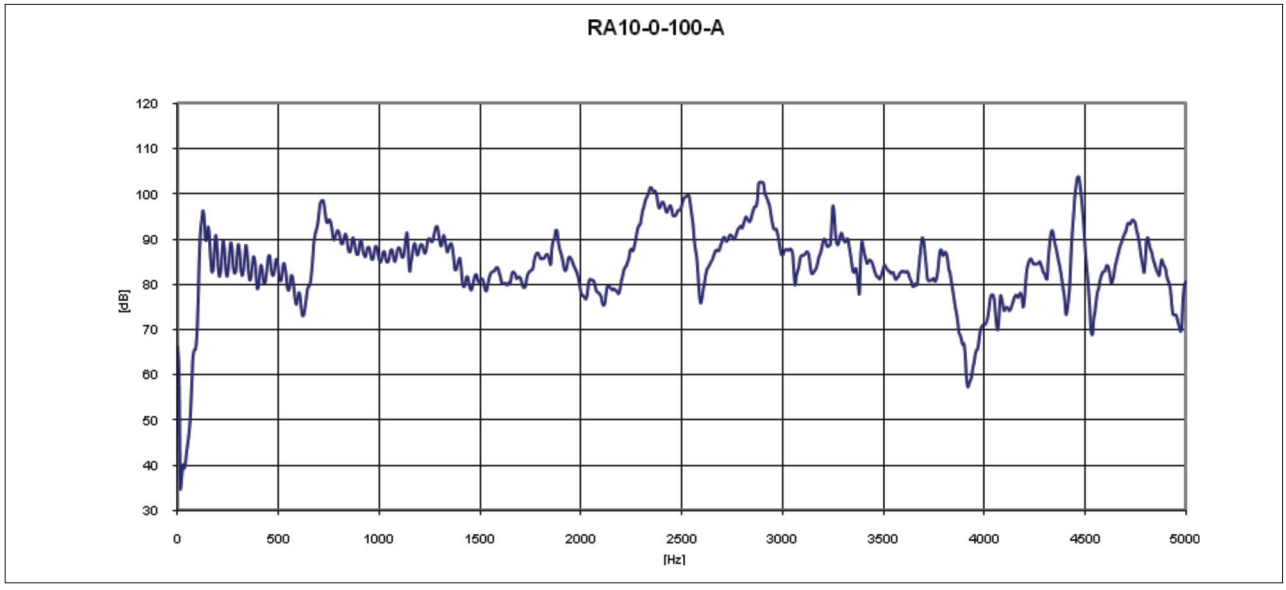

Figure 11: Transversal measurement – Configuration CFGB2

the other configurations, the resonances related to the longitudinal modes are easily identified. The theoretical *versus* experimental comparison presents 4.6% error for the first longitudinal mode and 2.9 and 11.7% for the second and third, respectively. Considering the averaged magnitudes, the measured longitudinal acoustic frequencies have 107, 102 and 92 dB. Table 6 depicts the results regarding the radial measurements. Considering the tangential modes, it is verified that the first acoustic frequency (1,105 Hz), calculated by Eq. 1, was not excited during the experimental tests. The second measured tangential frequency, when compared with the corresponding theoretical frequency, presented 21% error and its average magnitude was 103 dB. The radial modes presented 5.2 and 4.5% error, with average magnitudes of 103 and 98 dB, respectively. Finally, the coupled modes comparisons showed 4.1%, 0.7% and 6.4% errors.

Observe the FRF (Fig. 9 and Fig. 10) and note that these curves present noise below 500 Hz. This is due the low signal/noise ratio, since the generated acoustic noise (white noise) does not excite spectral components below the referred frequency, due to the manufacture characteristics of the acoustic source. As such, the measurement noises, inherent to the measurement chain, are also captured in low frequency.

Comparing Tables 3 and 4, we can verify the nozzle influence on the acoustic behavior of the combustion chamber cavity. Note the configurations B1 (without divergent) and B2 (long divergent) and verify that the obtained values of the first acoustic natural frequency do not change significantly. The second longitudinal frequency is approximately 40 Hz higher for the configuration B2, with long divergent. The third longitudinal mode of the configuration B2 is 25 Hz lower than the respective frequency of the configuration B1, without divergent. Other frequencies as tangential, radial and coupled can also be compared on these tables. Therefore, significant changes in the inner cavity acoustic behavior are not verified, when the nozzle length is increased.

CONCLUSIONS AND RECOMMENDATIONS

The procedures for evaluation of the acoustic resonances present a reasonable indication to identify these frequencies and their associated modes. Therefore, it may be considered that the mathematical model described in Eq. 1, with the inherent approximations and assumptions can be inaccurate, mainly for the higher orders modes. As such, it is important that theoretical calculations consider geometry variations for the determination of the acoustic natural frequencies of combustion chambers.

In view of better establishing the acoustic responses of the acoustic cavities, it is recommended that virtual prototypes be built up, using deterministic techniques as Finite Element Method (FEM) and Boundary Element Method (BEM), and acoustic analysis may be done to calculate the acoustic resonance frequency as well as to obtain their associated mode shapes, with more accurate models. Nevertheless, care must be taken with the limitations of these methods, since higher frequency analysis may consider a rule based on element discretization, which may be verified. Such rule states that an accurate model may present six to ten elements by wavelength, due to the relation between the wavelength and analysis frequency (Desmet and Vandepite, 2001).

Concerning the FRF measurements, the adopted procedure can be optimized for other configurations. As mentioned in this paper, transversal measures can be performed only for a few azimuth points as well as for only one radial point, because traveling acoustic waves assume plane wave behavior in the combustion chamber.

The identification and choice of the natural frequencies, for consequent association to the acoustic modes, despite presenting a reasonable indication by theoretical *versus* experimental comparisons, does not assure that these frequencies are the correct natural frequencies. Mainly for the tangential, radial and coupled modes, this identification and choice is a hard task, since it is done by visual analysis of the measured FRF as well as the average values of the magnitudes and frequencies. It is still important to consider the modal density of the FRF, which increases significantly when frequency increases, becoming the choice of the resonance peaks a difficult job.

The assessment of the influence of the nozzle length on the acoustic behavior of the acoustic cavity shows that such geometry alteration does not influence significantly the natural frequencies of the configurations B1 and B2.

A procedure indicated for experimental identification of the eigen-values and eigen-vectors of combustion chamber is the execution of the experimental modal analysis of the referred cavities. As such, transfer functions between input/output acoustic signals, measured by two microphones, can be obtained for the determination of the acoustic modal parameters (natural frequencies and mode shapes). Experimental acoustic modal analysis and theoretical acoustic modal analysis, calculated by deterministic tools, can be compared with the theoretical model validation and determination of the dynamic parameters of the combustion chamber cavity.

As described before, some modes in transversal (tangential and radial) directions were not acoustically excited or did not have enough energy generated to excite them satisfactorily. Such modes may be verified by exciting the cavity using pure tone signals. As such, all the energy of the signal is designated to excite the cavity in the required frequency.

The continuity of this combustion chamber instability survey may preview another research phase, in which acoustic noise passive insulation techniques should be applied. Such a way, baffles, filters and Helmholtz resonators may designed and with these devices attenuating or eliminating the sound pressure levels inside the chamber cavity, consequently eliminating possible combustion instabilities due to the coupling between acoustic modes and the combustion process. Once again, it is suggested that virtual prototypes may be used for design simulations and sensitivity analysis, with the different applicable apparatus.

REFERENCES

Burnley, V. S., Culick, F. E. C., 1997, "The influence of Combustion Noise on Acoustic Instabilities", Air Force Research Laboratory, OMB Nº 0704-0188.

Culick, F. E. C., 2000, "Combustion Instabilities: Mating Dance of Chemical, Combustion and Combustor Dynamics, American Institute of Aeronautics & Astronautics, A00-36437 in 36th AIAA/ASME/SAE/ASEE Joint Propulsion Conference and Exhibit, Alabama, USA.

Desmet, W., Vandepite, D., 2000, "Finite Element Method in Acoustic", Grasmech Course, Katholieke Universiteit Leuven.

Huzel, D. K., Huang, D.H., 1992, "Modern Engineering for design of liquid - propellant rocket engines", American Institute of Aeronautics and Astronautics.

Laudien, E., Pongratz, R., Piero, R., Preclik, D., 1995, "Experimental Procedures Aiding the Design of Acoustic Cavities", in: V. Yang, W. E. Anderson (Eds.), Liquid Rocket Engine Combustion Instability, Vol. 169, chap. 14, Progress in Astronautics and Aeronautics, AIAA, Washington, DC, pp. 377-399.

NASA, 1974, "Rocket Engine Combustion Stabilization Devices", NASA Space Vehicle Design Criteria (Chemical Propulsion), NASA SP8113.

Gerges, S. N. Y., 2000, "Ruído, Teoria e Fundamentos", NR Editora, ISBN 85-87550-02-0.

Santana Jr., A., et al., 2009, "Acoustic Cavities Design Procedures" Engenharia Térmica, Vol. 6, pp. 27-33.

Sutton, G. P., Biblarz, O., 2001, "Rocket Propulsion Elements", New York, John Wiley & Sons.

Yang, V., Wicker, J. M., Yoon, M. W., 1994, "Acoustic Waves in Combustion Chambers", Liquid Rocket Engine Combustion Instability, Progress in Astronautics and Aeronautics, Chapter 13, Vol. 169.